論文 / 著書情報
Article / Book Information

Title	Experimental Verification of Impact Absorbing Property of Wire Driven Joint with Synthetic Fiber Rope
Authors	Takuma Yabuta, Hiroyuki Nabae, Koichi Suzumori, Gen Endo
Citation	Proceedings of the 2020 IEEE/SICE International Symposium on System Integration, Vol. , No. , pp. 1306-1311
Pub. date	2020, 1
Copyright	(c) 2020 IEEE. Personal use of this material is permitted. Permission from IEEE must be obtained for all other uses, in any current or future media, including reprinting/republishing this material for advertising or promotional purposes, creating new collective works, for resale or redistribution to servers or lists, or reuse of any copyrighted component of this work in other works.
DOI	http://dx.doi.org/10.1109/SII46433.2020.9026266
Note	This file is author (final) version.

Experimental Verification of Impact Absorbing Property of Wire Driven Joint with Synthetic Fiber Rope

Takuma Yabuta[1], Hiroyuki Nabae[1], Koichi Suzumori[1] and Gen Endo[1]

***Abstract*— In a quadruped robot, the impact force applied to the leg mechanism by falling or stepping over is a problem that may cause damage to the mechanism. Therefore, various systems to increase impact resistance have been studied. In order to have high impact resistance, there are methods to withstand the impact by using a high-rigidity drive system, such as hydraulic cylinders which is heavy and large, or methods to absorb it by control using back-drivable actuators which is low energy efficient for quadruped robot. On the other hand, various series elastic actuators have been studied, which can absorb impact. Meanwhile, we have been studying synthetic fiber wire drive system. Synthetic fiber wire drive system is lightweight and can handle actuator arrangement freely. Also, synthetic fiber rope has elasticity, and if the elongation of the wire is measured and the force is estimated by its elastic characteristic, impact absorption and torque control can be performed. In this paper, we firstly compare the impact absorption of wire drive mechanism to that of harmonic drive mechanism as a typical reduction mechanism. For comparison, we build a 1 DoF link mechanism for both drive mechanism, and compare impact absorption by drop weight test. Then, a control to absorb the impact by measuring the elongation of the wire and estimating the force applied to the link is performed and evaluated with the link mechanism with fix axis replaced with a motor. The gain of position control was regulated by the estimated force applied to the link in order to back drive the motor and to absorb impact force. As the result, comparing with the harmonic drive link mechanism, the wire driven link mechanism can reduce impact force by approximately 66%. Also, the impact force can be reduced by approximately 10% by the impact absorption system.**

I. INTRODUCTION

Quadruped robots have to survive high force impacts during operation, resulting from falling down of surfaces, jumping, and stepping over obstacles (Fig. 1). Therefore, various research is being conducted in the field of impact resistance of quadruped robots. In order to increase the impact resistance, high-rigidity drive systems and back-drivable actuators for impact absorption are being developed. An example of a high-rigidity drive system is a hydraulic cylinder, such as the one employed in TITAN-XI [1]. However, driving with hydraulic cylinders tends to increase the mass of the system, making it difficult to construct a compact robot. Examples of robots with back-drivable actuators include the hydraulic humanoid robot Hydra [2] and the quadruped robot MIT Cheetah [3], which combines an electric motor with a lower reduction speed ratio. However, the hydraulic systems are heavy, and the energy efficiency of electro motors are greatly reduced if they are equiped with a lower reduction speed ratio. In addition, the motor plus lower reduction speed ratio configuration always requires torque to maintain the posture, resulting in energy consumption when the quadruped robot is used as a stable scaffold. Therefore, various elastic actuators, such as the high reduction ratio electric actuator plus elastic element, have been studied [4] [5]. For example, the HEBI Robotics actuator unit X-Series Actuators [6] [7] implements a mechanism that absorbs impact by deformation of rubber installed in the final output stage. Furthermore, the deformation of the rubber element is also used for controlling the torque.

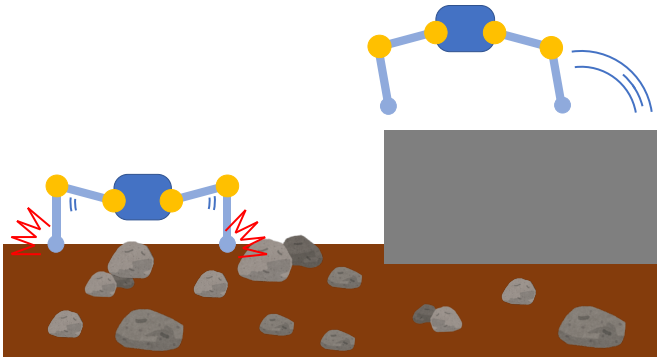

Fig. 1: Image of falling down

Meanwhile, we have been studying using a synthetic fiber rope drive system [8] [9]. The advantages of this type of drive system are that the actuator can be freely arranged, it is inherently lightweight, and that it can be easily and inexpensively replaced as a mechanical component. Fig. 2 shows an example of synthetic fiber wire drive system used in TITAN-XIII [10]. TITAN-XIII is a energy efficient quadruped robot with a low-inertia leg mechanism. We considered even if a new elastic element is not added, if the elasticity of a synthetic fiber wire can be utilized and its elongation by applied force can be measured, impact absorption and torque control can be performed like a series elastic actuator. Therefore, the goal of this research is to investigate the impact absorption characteristic and joint control with synthetic fiber wire drive system empirically. In this paper, the impact absorption of the synthetic fiber rope drive system is compared to a harmonic drive mechanism. Subsequently an impact absorption control method was developed and evaluated using the synthetic fiber rope elongation during impact.

[1]Takuma Yabuta, Gen Endon, Koichi Suzumori and Hiroyuki Nabae are with the Department of School of Engineering, Tokyo Institute of Technology, 2-12-1 Ookayama Meguroku, Tokyo, 152-8552, Japan yabuta.t.ab@m.titech.ac.jp

Fig. 2: TITAN-XIII, Kitano et al. [10]

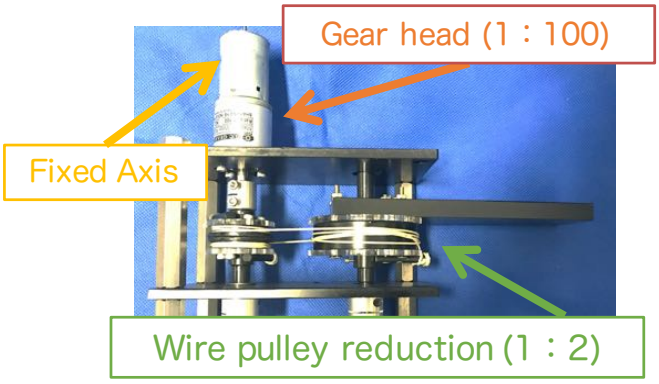

Fig. 3: Synthetic fiber rope drive with fixed axis

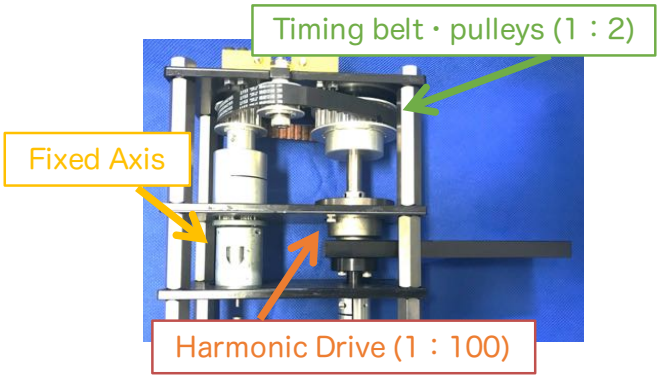

Fig. 4: Harmonic drive system with fixed axis

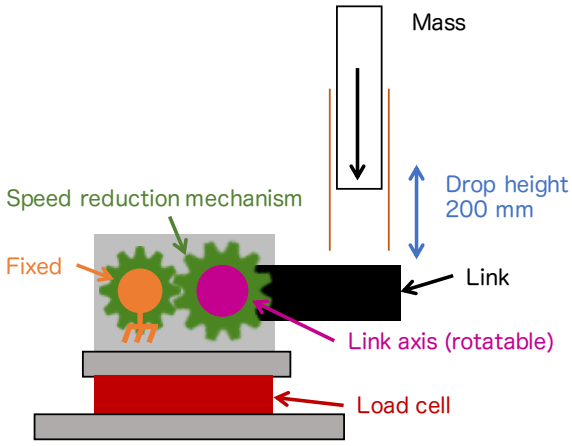

Fig. 5: Experimental setup of the impact experiments

II. COMPARISON EXPERIMENT BETWEEN WIRE DRIVE SYSTEM AND HARMONIC DRIVE SYSTEM

First, we evaluated to which extent the synthetic fiber rope drive system itself has impact-absorbing characteristics and compared this to other drive systems. For this purpose, it is compared with a harmonic drive which is typical reduction gear. Two different link mechanisms were manufactured: 1) a link mechanism with a synthetic fiber rope reducer /drive system and 2) a link mechanism with a harmonic drive system / reducer. Both link mechanisms are exerted to the same impacts and evaluated on the magnitude of the impact peak force measured by the load cell. From the impact peak force the impact absorption is calculated.

A. LINK MECHANISM

A one-degree-of-freedom link mechanism was fabricated in order to compare the impact absorption of the synthetic fiber rope drive system and the harmonic drive drive system, see Fig. 3 and Fig. 4, respectively. Synthetic fiber ropes made of Ultra High Molecular Weight Polyethylene (UHMWPE, Izanus, Hayami Industry Co.) were used for the wire drive system. UHMWPE was adopted for the wire drive mechanism because of its excellent repetitive bending durability [8] and high impact absorption [11]. The link mechanism is 85 mm in length and made of polyacetal. The reduction ratio in the force transmission from the link to the fixed shaft in both link mechanisms were set at 200.

B. EXPERIMENTAL SET-UP

A drop weight test was performed to measure the force applied to both link mechanism. Fig. 5 shows the conceptual diagram of the experimental setup. The orange circle indicates the fixed axis and the pink circle the link axis. The reduction gear shows the wire-pulley reducer, the gear head for both the wire-driven link mechanism and the harmonic drive and the timing belt-pulley reducer for the harmonic drive link mechanism. The impact was created by a 374 g weight which was dropped on the tip of link through guide-pipe from a height of 0.2 m. The load cell (CMM1-100K-CP, MinebeaMitsumi Inc.) was sandwiched between two aluminum plates. A linear motion guide was connected to the load cell to measure the force applied to the link mechanism. The output of the load cell was collected by a recorder (EDX-200A, KYOWA Electronic Instruments Co.), whose sampling frequency was set to 20 kHz, and whose low pass filter was set to 3 kHz.

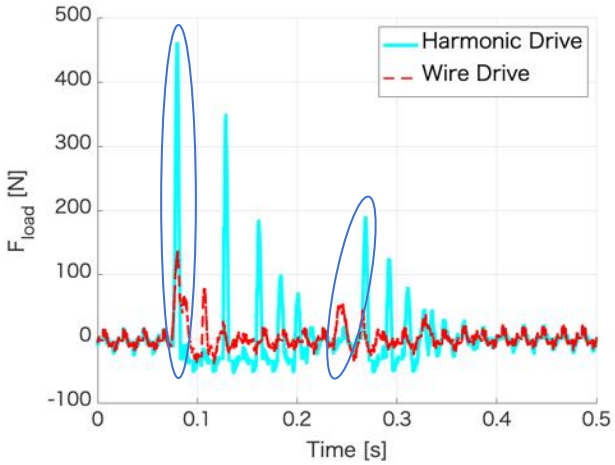

Fig. 6: Force versus time for the synthetic fiber rope and harmonic drive system. The blue circled peaks are the collision of weight.

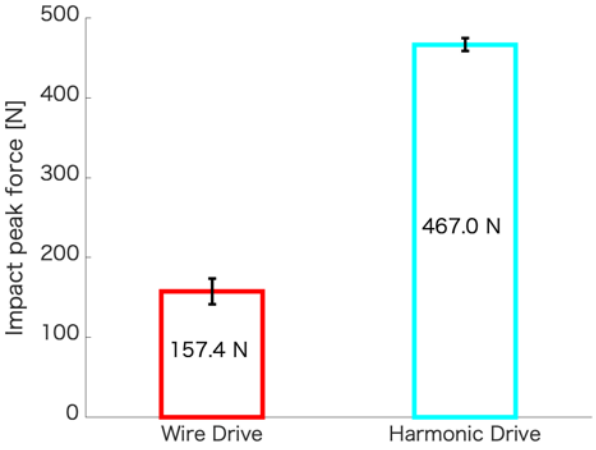

Fig. 7: Box plot of the average impact force of first peak of each link mechanism

C. RESULT

The impact experiment was carried out 5 times for each link mechanism. Fig. 6 shows impact experiment results of synthetic fiber rope drive system and harmonic drive system where F_{load} is the force measured the load cell. The dotted line indicates impact force experienced by the synthetic fiber rope drive system and the solid line indicates the impact load as experienced by the harmonic drive system. The small periodic vibration measured before and after the impact is noise of the load cell. The blue circled peaks are the collision of weight, whereas the other peaks are the weight bouncing on the link mechanism and the aluminum plate on the load cell. Comparing the amplitude of the first and second impact force peaks, synthetic fiber rope drive system can absorb the impact faster than the harmonic drive system. The peak impact force of the synthetic fiber rope drive system was 157.4 N, whereas an impact force of approximately 467.0 N was measured in the harmonic drive system, as illustrated in Fig. 7. In other words, the synthetic fiber rope drive system is able to reduce the impact force by approximately 66% compared to the harmonic drive system.

III. EVALUATION EXPERIMENT OF IMPACT ABSORPTION CONTROL

In the previous section, the impact-absorbing characteristic of synthetic fiber wire drive system was evaluated. In an effort to further increase the impact-absorbing characteristic, we designed and evaluated an impact absorption control that changes the gain by the applied force based on the elongation of synthetic fiber rope during impact. The impact absorption control method is based on the elasticity of the synthetic fiber rope. For evaluating the applied force, we developed a link mechanism which can measure the elongation of the synthetic fiber rope drive system and the spring constant of the synthetic fiber rope.

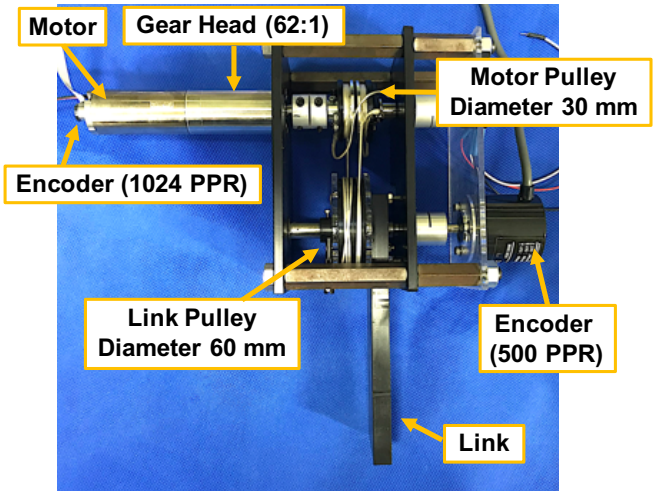

Fig. 8: Overview of the wire driven link mechanism

A. LINK MECHANISM

For this experiment we reused the previously developed link mechanism, with one major alteration. Instead of the fixed axis, a geared motor was used, see Fig. 8. The motor (B7A1E9E33A2C, MAXON MOTOR) has gear head reduction ratio of 62, resulting in a total reduction ratio of the link mechanism of 124. The resolution of the encoder attached to the link axis is 0.18 deg and that of the motor pulley's axis rotation is 1.42×10^{-3} deg. For calculating wire stretch by rotation of both axes, we adjusted the rotation resolution of the motor pulley's axis to 0.32 deg, to ensure that the resolution of the motor pulley axis is equal to that of the link axis.

B. MEASUREMENT OF SPRING CONSTANT

In order to estimate the force applied to the link by measuring the elongation of wire, it is necessary to know the spring constant of the UHMWPE rope in the mechanism. In order to determine the spring constant, we loaded and

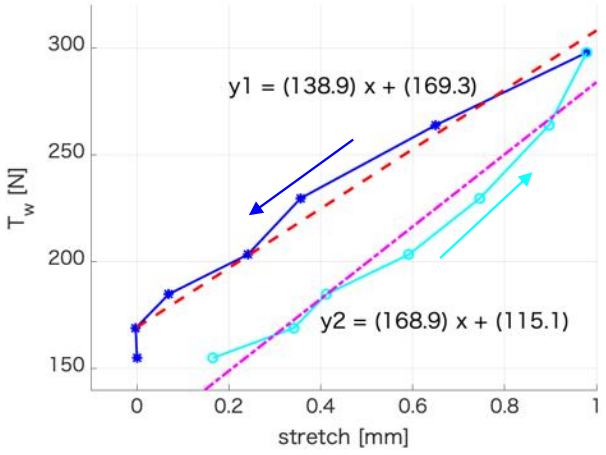

Fig. 9: Measurement of wire spring constant. The light blue line indicates measurement of loading weight, and the blue line indicates measurement of unloading weight.

unloaded weights on the link and measured the stretch of wire using the encoder. This experiment was repeated two times. In this experiment, a fixed axis was installed instead of the described motor. The stretch of wire, Δl, is calculated as follow:

$$\Delta l = -r_{mp}\theta_{mp} + r_{lp}\theta_l \tag{1}$$

where r_{mp} is the radius mm of the motor pulley, θ_{mp} is the rotation angle rad of the motor pulley axis which was 0 deg at this time, r_{lp} is the radius mm of the link pulley and θ_l is the rotation angle of the link axis.

The solid lines in Fig. 9 show a tension-stretch data of one of 2 measurement trials. We applied a tension of 150 N to the wire by hanging two weights with a mass of 5.14 kg on the link, 85 mm from its rotational center. The wire tension T_w is given by

$$T_w = \frac{MgL_p}{r_{lp}} + T_{init} \tag{2}$$

where M is mass [kg], g is gravitational acceleration, L_p is the distance between hanging point on link and the rotation center [mm] and T_{init} is initial tension [N] of wire. From Fig. 9, we find the hysteresis loop. The dotted magenta line in Fig. 9 illustrates the linear approximation of loading curve, and the dotted red line illustrates the linear approximation of unloading curve. As can be seen from the hysteresis loop, it is too difficult to measure force applied to the link by measuring elongation of wire with the encoders. Therefore, we decided to use the average slope of the loading and unloading cycle and use a linear approximation as wire spring constant for the mechanism to roughly estimate the applied force. The slope values of each measurement was calculated in the same way as illustrated above and are shown in Table I. From the table, an average spring constant of 1.74×10^2 N/mm was calculated.

TABLE I: Slope values [N/mm] of measurement data

	loading weight	unloading weight
Measurement1	1.69×10^2	1.39×10^2
Measurement2	2.33×10^2	1.56×10^2

TABLE II: Values of Gains

K_p	0.1
K_i	0.3

C. IMPACT ABSORPTION CONTROL METHOD

We designed impact absorption by regulating the gain based on the estimated force applied to the link, which in turn is estimated based on the previously deducted spring constant of the synthetic fiber rope. The force applied to the link is estimated from the difference between the link axis rotation angle (derived from the encoder value on the link axis) and the motor pulley axis rotation angle calculated with the encoder value on the motor and the spring constant, k_{wire} as follow:

$$F_{link} = k_{wire}(r_{lp}\theta_l - r_{mp}\theta_{mp})\frac{L_{link}}{r_{lp}} \tag{3}$$

where L_{link} is the length of the link (130 mm). For controlling the link angle, PI control was performed on the position, and the gain was regulated by multiplying the gain based on the force applied to the link. When the gain was calculated according to the estimated force, a dead zone of 35 N was provided for the force in consideration of the resolution of the encoders. The gain G_f is calculated with the estimated force, F_{link} as follow:

$$G_f = \begin{cases} 1 & (|F_{link}| < f_0) \\ \frac{1}{1+H_p(|F_{link}|-f_0)+H_d\left|\frac{\delta(F_{link}-f_0)}{\delta t}\right|} & (|F_{link}| > f_0) \end{cases} \tag{4}$$

where f_0 is 35 N as dead zone, H_p is proportional gain, and H_d is derivative gain. The reason why the Eq. 4 was established is explained qualitatively. $H_p(|F_{link}| - f_0)$ is a proportional term. $H_d\left|\frac{\delta(F_{link}-f_0)}{\delta t}\right|$ is a term related to the time variation of force. In order to reduce the impact peak force, the gain should become small before impact peak force is detected. Therefore, we considered that implementing the derivative term may regulate the gain quickly. Operation value, U is computed with the gain, G_f, and PI position control as follow:

$$U = \left(K_p e(t) + K_i \int e(t)dt\right) G_f \tag{5}$$

where K_p is the proportional gain for position, $e(t)$ is error value of position, and K_i is the integral gain for position. The selected gains are illustrated in Table II. The other gains were experimentally determined using three control cases, see Table III. This method lets the link mechanism back drive by making the control input smaller by reducing rigidity of link, reducing the impact peak force.

TABLE III: Values of Gains for each experiment

	Case 1	Case 2	Case 3
H	1, 0.5, 0.1, 0.05, 0.01, 0	1	1
H_p	0	1, 0.1, 0.01	0
H_d	0	0	0.01, 0.001, 0.0001

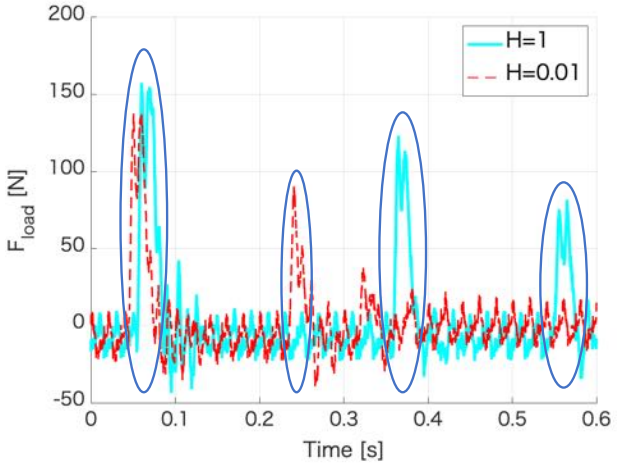

Fig. 10: Obtained load cell data from the impact experiment. The blue circled peaks are the collision of weight.

D. EXPERIMENTAL SET-UP

The experimental setup is similar to the one illustrated in Fig. 5, with two major differences. Instead of fixed axis, the geared motor was installed, and the link length was changed to 130 mm. The impact force was delivered by a weight of 855 g that was dropped onto the link from a height of 0.2 m. The output of the load cell was collected by a recorder set at a 50 kHz sampling frequency and using 3 KHz low pass filter.

E. RESULT

The control frequency was set to 2 kHz. The experiment was repeated six times. Fig. 10 shows case 1 results where F_{load} is the applied force measured with the load cell. The dotted line indicates the time history of the force measured by load cell with $H = 1$ and the solid line is the time history of the force measured by load cell with $H = 0.01$, and the blue circled peaks are the collision of weight. Because of bounding weight, there are large peaks after first peak. When comparing the amplitude of the impact peak forces, the system with a small gain can suppress the impact faster than the system with a large gain. The peak impact force of case 1 are shown in Fig. 11. As can be seen, reducing the gain H, in turn reduces the impact peak force. The peak value of impact force increased to 171.6 N when H was set to 0. That is because the motor driver (HB-UM-1XH-0814, HiBot Corporation) is only able to control a duty ratio of in between 95% and 5%. The result of case 2 and case 3 are shown in Fig. 12 and Fig. 13, respectively. According to Fig. 12 and Fig. 13, changing H_p, as well as changing H_d can reduce the peak of impact force by approximately

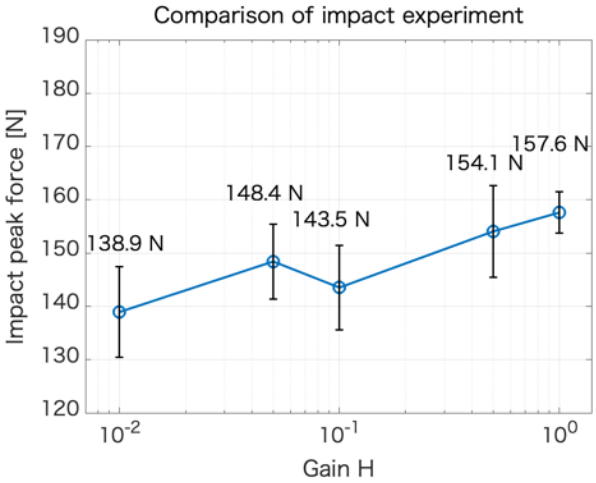

Fig. 11: Average impact peak force versus the gain H in case 1

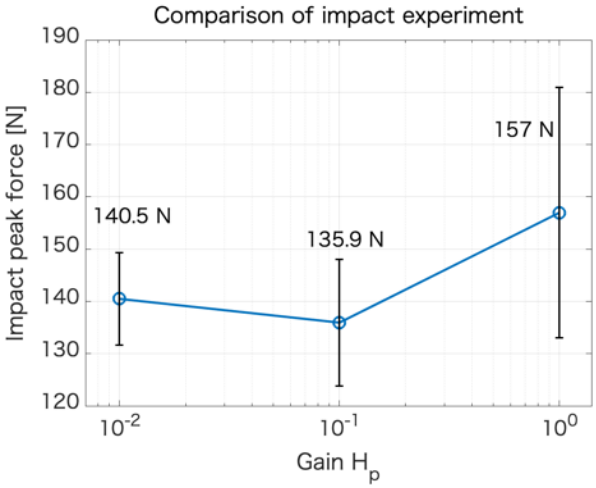

Fig. 12: Average impact peak force versus the gain H_p in case 2

10%. Considering Eq. 4, when H_p and H_d are large, G_f gets small. However, the results show that the largest impact force occured when H_p and H_d are the largest values. In case 1, the duty ratio was lower than 5% with $H_p = 1$ and $H_d = 0.01$.

IV. CONCLUSION

The impact absorption of the wire drive mechanism using synthetic fiber rope was compared to that of an harmonic drive mechanism. It was found that the wire drive mechanism reduced the impact force by approximately 66%. Subsequently, we implemented an impact absorption control method from the elongation to absorb the impact to the link mechanism and evaluated it. The control method reduced the impact force even further by approximately 10%. In the future, we will evaluate the relationship between the impact absorption and gear head versus wire-pulley reduction ratio. And we shall examine the applicability of the impact

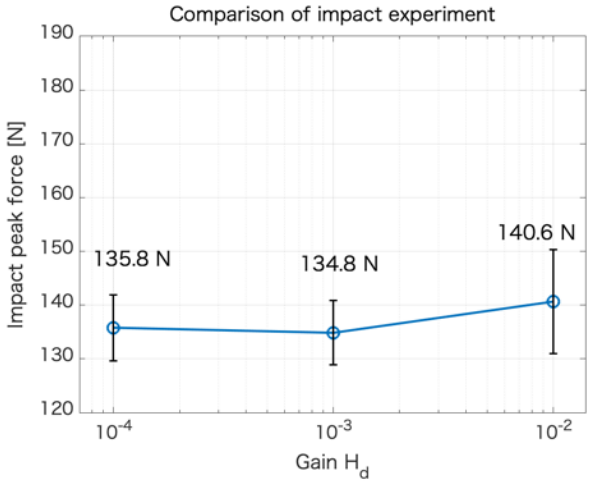

Fig. 13: Average impact peak force versus the gain H_d in case 3

absorption method to a quadruped robot driven by high tensile strength synthetic fiber ropes.

REFERENCES

[1] R. Hodoshima, T. Doi, Y. Fukuda, S. Hirose, T. Okamoto, and J. Mori, "Development of titan xi: a quadruped walking robot to work on slopes," in *2004 IEEE/RSJ International Conference on Intelligent Robots and Systems (IROS) (IEEE Cat. No.04CH37566)*, vol. 1, Sep. 2004, pp. 792–797 vol.1.

[2] T. Ko, K. Yamamoto, K. Murotani, and Y. Nakamura, "Compliant biped locomotion of hydra, an electro-hydrostatically driven humanoid," in *2018 IEEE-RAS 18th International Conference on Humanoid Robots (Humanoids)*, Nov 2018, pp. 280–283.

[3] P. M. Wensing, A. Wang, S. Seok, D. Otten, J. Lang, and S. Kim, "Proprioceptive actuator design in the mit cheetah: Impact mitigation and high-bandwidth physical interaction for dynamic legged robots," *IEEE Transactions on Robotics*, vol. 33, no. 3, pp. 509–522, June 2017.

[4] G. A. Pratt and M. M. Williamson, "Series elastic actuators," in *Proceedings 1995 IEEE/RSJ International Conference on Intelligent Robots and Systems. Human Robot Interaction and Cooperative Robots*, vol. 1, Aug 1995, pp. 399–406 vol.1.

[5] W. M. dos Santos, G. A. Caurin, and A. A. Siqueira, "Design and control of an active knee orthosis driven by a rotary series elastic actuator," *Control Engineering Practice*, vol. 58, pp. 307 – 318, 2017. [Online]. Available: http://www.sciencedirect.com/science/article/pii/S0967066115300198

[6] HEBI Robotics. (2019, Aug.) X-series actuators. [Online]. Available: https://www.hebirobotics.com/x-series-smart-actuators

[7] D. Rollinson, Y. Bilgen, B. Brown, F. Enner, S. Ford, C. Layton, J. Rembisz, M. Schwerin, A. Willig, P. Velagapudi, and H. Choset, "Design and architecture of a series elastic snake robot," in *2014 IEEE/RSJ International Conference on Intelligent Robots and Systems*, Sep. 2014, pp. 4630–4636.

[8] A. Horigome and G. Endo, "Investigation of repetitive bending durability of synthetic fiber ropes," *IEEE Robotics and Automation Letters*, vol. 3, no. 3, pp. 1779–1786, July 2018.

[9] A. Takata, G. Endo, K. Suzumori, H. Nabae, Y. Mizutani, and Y. Suzuki, "Modeling of synthetic fiber ropes and frequency response of long-distance cable–pulley system," *IEEE Robotics and Automation Letters*, vol. 3, no. 3, pp. 1743–1750, July 2018.

[10] S. Kitano, S. Hirose, G. Endo, and E. F. Fukushima, "Development of lightweight sprawling-type quadruped robot titan-xiii and its dynamic walking," *2013 IEEE/RSJ International Conference on Intelligent Robots and Systems (IROS)*, November 2013.

[11] V. Sry, Y. Mizutani, G. Endo, Y. Suzuki, and A. Todoroki, "Consecutive impact loading and preloading effect on stiffness of woven synthetic-fiber rope," *Textile Science and Technology*, vol. Vol.3, no. No.1, 2017.